Published in final edited form as:
IEEE Trans Biomed Eng. 2012 March ; 59(3): 717–727. doi:10.1109/TBME.2011.2178411.

Instantaneous Measure of EEG Channel Importance for Improved Patient-Adaptive Neonatal Seizure Detection

Andriy Temko [Member, EMBS], **Gordon Lightbody**, **Eoin Thomas**, and **William Marnane [Member, EMBS]**
Department of Electrical and Electronic Engineering and the Neonatal Brain Research Group, University College Cork, Ireland

Andriy Temko: andreyt@eleceng.ucc.ie; Gordon Lightbody: g.lightbody@ucc.ie; Eoin Thomas: eoint@eleceng.ucc.ie; William Marnane: l.marnane@ucc.ie

Geraldine Boylan
Department of Pediatrics and Child Health and the Neonatal Brain Research Group, UCC, Ireland

Geraldine Boylan: g.boylan@ucc.ie

Abstract

A measure of bipolar channel importance is proposed for EEG-based detection of neonatal seizures. The channel weights are computed based on the integrated synchrony of classifier probabilistic outputs for the channels which share a common electrode. These estimated time-varying weights are introduced within a Bayesian probabilistic framework to provide a channel-specific and thus adaptive seizure classification scheme. Validation results on a clinical dataset of neonatal seizures confirm the utility of the proposed channel weighting for the two patient-independent seizure detectors recently developed by this research group; one based on support vector machines and the other on Gaussian mixture models. By exploiting the channel weighting, the ROC area can be significantly increased for the most difficult patients, with the average ROC area across 17 patients increased by 22% (relative) for the SVM and by 15% (relative) for the GMM-based detector, respectively. It is shown that the system developed here outperforms the recent published studies in this area.

Keywords

Neonatal; Seizure; Detection; EEG; Channel; Selection; Weighting; Montage; Classification; Probability

I. Introduction

Seizures in newborn babies are commonly caused by problems such as lack of oxygen, haemorrhage, meningitis, infection and stroke. The incidence of clinically apparent neonatal seizures is generally reported as around 3 per 1000 and under certain circumstances, such as in very preterm babies, 50 per 1000 [1]. In reality, these values are probably underestimates as approximately one third of all seizures are clinically visible and many remain undetected in the busy Neonatal Intensive Care Unit (NICU) [2]. Failure to detect seizures and the resulting lack of treatment can result in brain damage and in severe cases, death. A system that could automatically detect and annotate seizures on the neonatal EEG would be extremely useful to clinicians in the NICU. Although a number of methods and algorithms have been previously proposed in an attempt to automatically detect neonatal seizures [3] – [5], to date their transition to clinical use has been limited due to poor performance.

Europe PMC Funders Author Manuscripts

Clearly, the performance of the seizure detection systems depends on the information content of the corresponding EEG channels. By using as many channels as possible one minimizes the probability that useful information is missed. On the other hand, it becomes more difficult to automatically find what information is useful in the available channels. Channel selection has been widely used in Brain Computer Interfaces (BCI) [6] – [13] mainly for the purpose of computational load reduction. In [11], five out of 64 channels were selected based on EEG synchronization likelihood, with a slight decay in performance reported for the task of emotion recognition. In [12], a method based on common spatial patterns was introduced to reduce the computational cost of a motor imagery task. For this type of task, the relevant EEG electrodes that lead to good classification results were identified in [9] and [13]. Indeed, a constant (in time) importance of information captured by a channel can be assumed for these tasks, especially when patient-specific classification systems are targeted [6], [9] – [13]. In [9], a recursive channel elimination procedure was applied by analogy with recursive feature elimination (RFE) [14] that is typically used for feature selection for Support Vector Machines (SVM). When the extracted features from all channels are concatenated to form a long feature vector prior to feeding the classifier, the channel selection problem can be tackled with the existing feature selection routines such as RFE [7], [9], mutual information criterion [8], or using other empirically derived criteria [10]. In this form, however, the classifier inherits dependencies between an event and its common location, which in addition, are patient-specific.

Patient-specific neonatal seizure detection has limited clinical utility. In fact, samples of testing patient data are never available beforehand in the NICU. Although neonatal seizure may generalize, many remain focal or multi-focal [15], that is, (highly) localized in different parts of the brain depending on the patient (Fig. 1, left). Because the dependencies between a seizure event and its common location are patient-specific, they cannot be learnt in a supervised way. Additionally, neonatal seizures can migrate from one brain zone to another in a non-ordered fashion (Fig. 1, right). Both observations increase the chances that a seizure will be missed in a pre-selected subset of channels. As such, a channel selection procedure which is dynamic, i.e. changing in time, would be very useful. Channel weighting can be seen as a generalization of channel selection, where the weights can take values other than binary.

Two patient-independent neonatal seizure detectors have recently been developed by this research group [16], [17]. The neonatal seizure detection systems developed so far exploit the same channels, in the bipolar montage, which are used by clinicians to annotate the data. However, highly-localized seizures in several of the most difficult patients still account for errors as shown in [18]. This work aims at using all available channels and dynamically weighting them to emphasize the relevant information. In particular, this work first formulates the neonatal seizure detection problem in probabilistic terms using a Bayesian framework [19] to help indicate where such weighting terms should be used. A methodology for the estimation of the time-varying channel weights based on the synchronized energy of the primary classifier probabilistic outputs is proposed. Then, as the second step, the probabilistic output of these detectors for each channel is multiplied by the estimated time-varying weights. By emphasizing the patient-specific time-varying seizure locations, the detectors manage to self-adapt to every testing patient on-the-fly. The experiments are conducted on one of the largest clinical databases available in the area, which totals 267 hours in duration. The patient-independent leave-one-out (LOO) performance assessment is carried out with and without channel weighting and compared for two different classifiers and various sets of channels selected by sequential backward elimination (SBE) and sequential forward selection (SFS).

The paper is organized as follows: Section II briefly describes the neonatal seizure detectors previously developed by the group. Section III proposes a Bayesian formulation of seizure detection problem in a chosen channel. An approximation of the probabilistic terms related to the channel weighting is proposed in Section IV. Section V presents the experimental setup and comparison results, with and without channel weighting. Conclusions are drawn in Section VI.

II. Neonatal Seizure Detectors

A. Dataset

The dataset is composed of EEG recordings from 17 newborns obtained from NICU, Cork University Maternity Hospital, Cork, Ireland. The patients were full term babies ranging in gestational age from 39 to 42 weeks. All newborns had seizures secondary to hypoxic ischemic encephalopathy (HIE). A Carefusion NicOne video EEG machine was used to record multi-channel EEG at 256Hz using the 10-20 system of electrode placement modified for neonates (Fig. 2). As a standard of neonatal care [20], the following 9 active electrodes were used to record the data: T4, T3, O1, O2, F4, F3, C4, C3, and Cz. Then, the following 8 EEG channels in bipolar pair were used to annotate the data: F4-C4, C4-O2, F3-C3, C3-O1, T4-C4, C4-Cz, Cz-C3 and C3-T3. All seizures were annotated independently by two experienced neonatal electro-encephalographers using video EEG. All disagreements in annotations were resolved by consensus. The combined length of the recordings totals 267.9h and contains 705 seizures, which makes this dataset one of the largest in the neonatal area. The dataset contains a wide variety of seizure types including both electrographic-only and electro-clinical seizures of focal, multi-focal and generalized types. The continuous EEG recordings were not edited to remove the large variety of artifacts and poorly conditioned signals that are commonly encountered in the real-world NICU environment. The dataset used is detailed in Table I.

B. Automated seizure detection system architecture

The diagram of the systems is shown in Fig. 3. The EEG from the 8 above-mentioned channels was down-sampled from 256Hz to 32Hz with an anti-aliasing filter set at 12.8Hz. The EEG was then split into 8s epochs with 50% overlap between epochs. Fifty-five features were extracted from each channel which represent both time and frequency domain characteristics as well as information theory based parameters. These features are listed in Table II. Every EEG channel is processed independently, therefore the extracted features are not concatenated. Various system architecture choices (such as window length/shift, features, etc) are detailed in [16], [17].

The training data for the classifier were first normalized anisotropically by subtracting the mean and dividing by standard deviation to assure commensurability of the various features. This normalizing template was then applied to the testing data. The normalized features extracted from each epoch were then fed to train a single SVM/GMM classifier.

For the seizure class representation, per channel annotations are required to indicate on which channels the seizure event occurs and thus which channels contain class discriminative information and should therefore be used in training. In this work, 2 minutes of seizure per patient were annotated on the per-channel basis, indicating the involved channels. These 2 minutes were selected by a clinical neurophysiologist, with the only criteria being that there had to be clear seizure activity and that they should cover most seizure morphologies and variations. Sections of several independent seizures can contribute to these 2 minutes and indeed the set of the affected channels can vary for each section of seizure activity. In our performance assessment, which is explained later in Section II.C, the number of seizure feature vectors for training ranged from a minimum of 1507 to a

maximum of 1745. For the non-seizure class, 10,000 non-seizure feature vectors were randomly selected from all channels in the training dataset.

Two classifiers were implemented: an SVM with a Gaussian kernel and a GMM classifier with linear discriminant analysis feature preprocessing. Model selection on the training data was performed for both classifiers to choose suitable model parameters such as kernel hyper-parameters for SVM, or the number of Gaussians, covariance type, and the number of retained LDA components for GMM. For the SVM, on average 19% of the training data were retained as support vectors. The most frequent pair of selected hyper-parameters was γ=0.05 and C=20.

Neonatal seizures can be localized to a single EEG channel; for this reason the system was designed to process and classify each EEG channel independently. Thus, in the testing stage, the obtained classifier was applied separately to each channel of the testing data as shown in Fig. 3. The outputs of the SVM/GMM were converted to probability-like values (for the SVM-based system, it is done with a sigmoid function [21]) and smoothed with a moving average filter. The averaged value was then compared to a threshold from the interval [0 1]. After comparison, binary decisions were taken per channel: 1 for seizure and 0 for non-seizure. The binary decisions were then fused as follows: if there was a seizure in at least one channel, the whole epoch was marked as a seizure, otherwise it is denoted as a non-seizure. The ‘collar’ technique was applied last – every seizure decision was extended from either side to account for the delay introduced by the moving average filter and to compensate for possible difficulties in detecting pre-seizure and post-seizure parts. The post-processing steps make the system applicable to any number of EEG channels which can be very beneficial in clinical practice [16].

Both systems result in similar performance and significantly outperformed the existing alternatives as shown in [17], [18]. Detailed information on the systems can be found in [16], [17].

The same set of SVM and GMM models as in [16], [17] is used in this work. However, in contrast to those works, in the present study, the designed systems were tested on all 36 channels obtained from a bipolar montage of 9 electrodes. Thus, 24 EEG channels were not used in training as no annotations were available for those channels. The montage mismatch between training and testing data results in different levels of energy of incoming signals which were mainly attributable to the different distance between electrodes used in the montage [22]. Many features used in the system (such as sub-band energies, curve length, etc) incorporated information based on the absolute energy of the EEG signals used in training, thus making the system sensitive to the changes in signal energy levels. The histogram-based energy normalization technique proposed by the authors in [23] was therefore applied to all testing EEG signals to normalize their energy levels to that used in training.

C. Performance assessment and model selection

Patient-specific data is unavailable prior to seizure monitoring. For this reason, the LOO cross-validation method was used to assess the performance of the system for patient-independent seizure detection [18]. This way, all but one patients’ data was used for training and the remaining patient’s data was used for testing. This procedure was repeated until each patient had been a test subject and the mean result was reported. Several alternatives to the LOO performance assessment for neonatal seizure detection have been discussed in [18]. The LOO is known to be an almost unbiased estimation of the true generalization error [24]. What is examined with the LOO procedure is not a particular model, but indeed the methodology used to obtain such a model. This last point means that the LOO estimate

effectively gives a robust prediction of the performance that other researchers or practitioners will obtain using this method, but trained on their data. Here, seventeen 16 vs. 1 data splits made by the LOO method formed the performance assessment routine.

In each of these 17 times, the data from the 16 training subjects were only partially used for actual training of the primary classifier as only the data with the per-channel annotations were used to represent the seizure class while only 10000 epochs were selected to represent the non-seizure class. The data, which were not exploited for training the classifier, is called the development data in this study. The development data was used to tune other parameters in this work. This way, the model selection routine is completely independent of the performance assessment routine and the testing subject was not seen or used at any time for any system tuning.

D. Metrics and statistical tests

The metrics used in this work are epoch-based sensitivity and specificity values which are defined as the accuracy of each class (seizure and non-seizure) separately. In contrast to rule-based methods where a single operating point is achievable, the proposed system provides continuous, pseudo-probabilistic values. By thresholding the probability of seizure (in the range from 0 to 1), it is possible to report the curves of performance. The epoch-based Receiver Operating Characteristic (ROC) curve which plots sensitivity over specificity values is reported. The ROC area is related to the Mann-Whitney u-statistic test of significance [25]. This relationship can be used to derive statistical properties of the ROC area such as its standard error. To calculate the statistical significance of a difference between two algorithms (two ROC areas), the z statistic is computed by taking into account the correlation of the two ROC curves as suggested in [38]. The resultant p values of the two-tailed test are reported and values less than 0.05 are considered significant.

For comparison purposes, we also report the curve of the clinically-motivated event-based metrics – good detection rate (GDR) over the number of false detections per hour (FD/h).

III. Bayesian Inference For Seizure Detection Problem

As outlined, the obtained models can be applied to any EEG recording in a bipolar montage, so the previously-developed systems (Fig. 3) are channel-independent. In this section, a general neonatal seizure detection problem is first formulated in probabilistic terms using a Bayesian framework with no channel-specific information incorporated. Subsequently, channel context is introduced with channel-related weights placed.

Using Bayes' theorem, the posterior probability of having a seizure decision S given a feature vector $\mathbf{x}$ can be written as:

$$P(S|\mathrm{x}) = \frac{P(S)\,p(\mathrm{x}|S)}{P(\mathrm{X})} \quad 1$$

where $P(S)$ denotes a prior probability of having a seizure as annotated by clinical neurophysiologists, $p(\mathbf{x}/S)$ is a conditional probability (likelihood) that a feature vector $\mathbf{x}$ represents characteristics of a seizure class (S), and $P(\mathbf{X})$ represents a prior probability of all possible hypothesis and serves as a normalization constant. $P(\mathbf{X})$ can be calculated as the sum of the products of mutually exclusive hypotheses (S or NS) and corresponding conditional probabilities.

Equation (1) is already modeled by the existing detection systems. That is, for the SVM-based system, the sigmoid function [21], which is trained to convert the distances to

probability-like values, takes into account the priors of both classes. Thus, the output of the sigmoid function is a direct approximation of (1). For the GMM-based system, the likelihoods of both classes are explicitly generated and the priors are modeled separately based on the amounts of seizure and non-seizure in the training data annotations.

If the channel information is taken into account, the probability of a seizure for the channel c, given a new feature vector $\mathbf{x}$ can be computed, and then (1) can be rewritten as:

$$P(S|\mathrm{x},c)=\frac{P(S,c)\,p(\mathrm{x}|S,c)}{P(\mathrm{X},c)} \quad 2$$

where $P(S,c)$ is the joint prior probability of having a seizure S and it manifesting itself on channel c. $P(S,c)$ can be decomposed into having a channel-independent prior probability of a seizure $P(S)$, that is, the probability that the seizure occurs across any of the observed channels, and $P(c|S)$, that is, the probability that the seizure manifests on channel c given that the seizure occurs. Similarly, since the systems described in Section II use the designed models which are channel-independent, the likelihood generated by the model is also channel-independent. That is,

$$p(\mathrm{x}|S,c)\approx p(\mathrm{x}|S)\,P(c|\mathrm{x}) \quad 3$$

where $p(\mathbf{x}|S)$ is channel-independent likelihood from (1) and $P(c|\mathbf{x})$ is a data-dependent prior or weighting of channel c. Equation (2) can thus be expanded as:

$$\begin{aligned} P(S|\mathrm{x},c) &= \frac{P(S)P(c|S)p(\mathrm{x}|S,c)}{P(\mathrm{X},c)} \\ &= \frac{P(S)P(c|S)p(\mathrm{x}|S)P(c|\mathrm{x})}{P(\mathrm{X},c)} \end{aligned} \quad 4$$

which can be regrouped to yield,

$$P(S|\mathrm{x},c)=\frac{P(S)\,p(\mathrm{x}|S)}{P(X,c)}P(c|S)\,P(c|\mathrm{x}) \quad 5$$

The only differences between the original Bayesian formulation (1) and the formulation with regards to a given channel c given in (5) are the two new terms introduced: the prior probability, $P(c|S)$, that a given seizure will manifest itself on channel c and the data-dependent weight, $P(c|\mathbf{x})$, of importance of the channel c. Both these new terms are channel-specific. Additionally, the first prior probability term does not depend on the observation $\mathbf{x}$, that is, it does not change with time. Both terms can be combined to form a final weight for each channel. The proposed method to estimate a channel-related weight is explained in the next section.

IV. A Data-Driven Measure Of Channel Importance

As outlined in Section II, the data in our study are recorded with N=9 electrodes and annotated using 8 channels in the bipolar montage. Effectively, the bipolar montage is chosen by clinicians at the stage of data annotation. In our case, there are N*(N-1)/2 = 36 possible channels in the bipolar montage. For certain applications, however, such as BCI, up to 128 electrodes are recorded, which adds up to more than 8000 channels in the bipolar montage. In these applications, referential montage is justified and widely used. To make the proposed scheme montage independent and to cope with the large number of possible bipolar channels in our study, the importance of a given electrode e is modeled first. Then, the combined bipolar channel weight is obtained as described in Section IV.C.

A. Modelling P(e|x)

The data-driven estimate (at time t) of the 'importance' of the i^{th} electrode $P(e_i|\mathbf{x})$ can be estimated using the probabilistic output of the classifier on a feature vector $\mathbf{x}$ after the moving average filter (Fig. 3). For every electrode e_i, several channels which share this electrode in the bipolar montage are selected. The list of selected channels for each electrode is given in Table III. It can be seen, that to model the importance of a particular electrode, the channels which cover the brain zone around the electrode of interest are selected.

Let $\mathbf{y}_i(r)$ be a vector of probabilistic output at time r of selected channels which are considered to model the importance of the i^{th} electrode. The $P_t(e_i|\mathbf{x})$ for electrode i at time t is then expressed as:

$$P_t(e_i|\mathrm{x}) = \frac{\sum_{r=1}^{t} \mathrm{y}_i^T(r)\,\mathrm{Q}_i\,\mathrm{y}_i(r)\,/|\mathrm{y}_i(r)|}{\sum_{j=1}^{N}\left(\sum_{r=1}^{t} \mathrm{y}_j^T(r)\,\mathrm{Q}_j\,\mathrm{y}_j(r)\,/|\mathrm{y}_j(r)|\right)} \quad 6$$

where $N=9$ is the number of electrodes used in a recording, $|\mathbf{y}_k(r)|$ denotes the cardinality (here the number of channels associated with the k^{th} electrode, Table III) of vector $\mathbf{y}_k(r)$ and $\mathbf{Q_k}$ is a $|\mathbf{y}_k(r)|\times|\mathbf{y}_k(r)|$ square matrix of the form

$$\mathrm{Q}_k = \begin{bmatrix} 0 & 1 & 1 & \dots & 1 \\ 0 & 0 & 1 & \dots & 1 \\ \ddots & & & & \\ 0 & 0 & \dots & & 0 \end{bmatrix} \in \mathrm{R}^{|\mathrm{y}_k|\times|\mathrm{y}_k|} \quad 7$$

Essentially, the average of the product-moments or cross-correlation at 0^{th} lag between selected channels, which share the same electrode, is calculated here to obtain a measure of agreement between probabilistic activities in a certain electrode at a point in time, r. The cumulative sum in the numerator of (6) represents the integrated synchrony or common energy up to the current point in time, t. To assure a partition of unity of $P(e_i|\mathbf{x})$ over all possible $\mathbf{x}$, the cumulative sum for a particular electrode, e_i, is normalized by the common energy over all the electrodes.

The example of the proposed measure is shown in Fig. 4 for patient 1. For this patient, most seizures are localized in the O2 electrode, which is reflected in the increased integrated synchrony for this electrode. The normalized measure of importance, shown in the middle (on a logarithmic scale), indicates that channels which contain electrode O2 will be approximately 4 times more emphasized than the other channels. It is interesting to note that the nearest neighbors of the O2 electrode (electrodes O1 and T4; see Fig. 2), share the second and the third places for most of the time.

It can also be observed that the emphasis of the electrode O2 increases sharply during ictal activity (indicated by the expert seizure labels) and decreases slowly during interictial periods of time (e.g. epochs 3500-6000, 10000-16000). The slow decrease during interictal activity indicates that the measure of importance has a built-in forgetting factor. If no ictal activity occurs for a long time, the importance of all electrodes will converge to the equilibrium state – the same value for all electrodes.

The benefit of the proposed measure is two-fold. First, the integrated synchrony will be high when there is a synchronous rise in probability of seizure in all considered channels that share the chosen electrode. In turn, a synchronized high probability activity is indicative of a

seizure. Effectively, this measure emphasizes the electrode/location in the brain which had a history of suspected seizures. In other words, the measure incorporates the fact that any new seizures are more likely to happen at the location where seizures activity have been observed before. Second, slight channel preference can be attributed to non-seizure activity which resembles 'seizure-like' behavior, e.g. periodic lateralized epileptiform discharges. This EEG activity results in synchronous but not high probabilistic response of the classifier and thus long accumulated periods would be needed to emphasize a channel. In fact, long periods of this activity may be suggestive of the upcoming seizure in the same location [26].

B. Modelling P(e|S)

In contrast to the data-driven $P(e/\mathbf{x})$, the $P(e/S)$ is a probability that, given a seizure is occurring, it is visible in electrode e. It aims at emphasizing, *a priori*, electrodes in which seizures are mostly expected. Unlike the channel-independent prior, $P(S)$, which can be modeled based on the training data annotation, the electrode-dependent, $P(e/S)$ requires per-channel annotations which are not available. Thus, $P(e/S)$ is estimated here from the statistics found in the clinical literature.

Many studies report the distribution of the location of seizure onsets in conventional EEG [27] – [30]. However, only few discuss the visibility of a seizure in a particular channel. Additionally, it has been shown that the location of the seizure onset and the visibility of the seizure (what we are interested in) can differ significantly. For example, in [27], it has been shown that while 56% of seizures originated from the central region, as many as 78% of seizures were visible in that zone. In [28], it has been reported that the theoretical visibility of a seizure in the central zone is as high as 94%. In another study [29], it has been shown that 46% of seizures are visible in the Fp1, Fp2 zones which are close to F3, F4 in our montage. No data were found regarding the visibility of seizures in the temporal or occipital zones, and there are no premises to believe that a seizure is more visible in the occipital and temporal zones than in the frontal zone. Based on the data collected from the literature, the $P(e/S)$ is represented here as shown in Table IV.

C. Combined channel weight

As has been mentioned above, the channel selection can be seen as a particular case of channel weighting, where the weights are binary in nature. Thus, it would be beneficial to have a means of controlling the distribution of the channel weights and thus the strictness of channel weighting. This is achieved in our work by applying the *softmax* function:

$$w_i(t) = \frac{\exp\left(kP_t(e_i|\mathrm{x})\,P(e_i|S)\right)}{\sum_{j=1}^{N}\exp\left(kP_t\left(e_j|\mathrm{x}\right)P\left(e_j|S\right)\right)} \quad (8)$$

where t is the current time, N is the number of electrodes, k is a multiplication constant which controls the severity of weighting. If k is large, a single non-zero weight is obtained for the most important electrode and the scheme converges to channel selection, where only those channels which contain this electrode are selected. Hence, k is the only parameter that has to be chosen beforehand. In our experiments, k is estimated on the development data for every fold in the leave-one-out performance assessment. Although k can be different for each fold, values close to 4.5 for the SVM and close to 10 for the GMM-based system were generally obtained over the training data. The difference in k values for SVM and GMM is mainly attributable to different probabilistic outputs after moving average filter (Fig. 3) as a result of different ways of modeling $P(S)$ in (1) – a sigmoid approximation for SVMs versus data-driven modeling for GMMs.

The two terms $P(e/S)$ and $P(e|\mathbf{x})$ have been modeled so far for every electrode. Looking at the two electrodes associated with channel c, a final measure per channel in the bipolar montage, at time, t, is calculated as the maximum of the measures for the two constituent electrodes:

$$P(c|S)\,P(c|\mathrm{x}(t)) \approx \max_{e_i \in c} (w_i(t)) \quad (9)$$

By choosing the *max* function it is assumed that the seizure picked up by a certain electrode will propagate to all bipolar channels which share this electrode. Thus, (9) assures that the final measure of the channel importance inherits the largest of the weights of the two constituent electrodes.

After the weight is calculated in (9), it is used to estimate the final probability in (5). Specifically, the classifier probabilistic output in each channel (after the moving average filter, see Fig. 3) is multiplied by its estimated time-dependent channel weight. To calculate the normalization term $P(\mathbf{X},c)$ in (5), the electrode weights $w_i(t)$ in (8) and consequently final channel importance in (9) are calculated for the non-seizure class as well, by substituting $P(e/S)$ with $1\text{-}P(e/S)$ in (8).

The final probability of the seizure can be seen as a combination of the current evidence (current probability of the seizure) and current confidence (channel weight). The main contribution of this study is to introduce dynamic weights which vary in time according to the patient's previous history. The final decision is still dominated by the probabilistic output of the primary classifier which is then weighted by the channel confidence measure.

V. Results And Discussion

A. Single channel performance

First, to show the difficulty of the problem, the performance of the SVM-based seizure detection system reported in [16], without any channel weighting, is shown in Fig. 5 for every possible single channel choice in the bipolar montage. Having a baseline ROC performance of 96.3% for the 8 channels used for data annotation (see Fig. 1), the maximum achievable ROC using a single channel is 91.4% (C3-C4), followed by 88.9% (Cz-C4) and 88.4% (C3-Cz). As most neonatal seizures are localized in different parts of the brain, no single channel can provide satisfactory performance. It can also be seen from Fig. 5 that channels with central electrodes on average reach higher performance than channels with electrodes located in occipital, frontal or temporal zone. This fact confirms clinical observations [27] used to model $P(e/S)$ in Section IV.B.

B. The effect of channel weighting

To show the effect of the channel weighting for various channel subsets, a channel SBE and SFS are performed in a similar manner to that usually used for feature selection [31]. This procedure effectively provides nested subsets of channels. In the proposed seizure detection framework, the fusion of channels in the post-processing is done by logical 'OR'; the channels can therefore be considered as independent. In fact, both SBE and SFS in our case result in the same output. The performance with and without channel weighting is shown in Fig. 6 for the SVM-based and the GMM-based detectors. These figures can be read from left to right as SBE or from right to left as SFS. The resultant sequence of channels was obtained over the development data and then tested on the testing data. For the process of SBE, all 36 channels were included and one channel was eliminated at a time. The channel was chosen to be eliminated if the difference of performance of a current set of channels with and

without it led to the highest ROC improvement or the smallest ROC decrease over the development data. This eventually terminates with the 8 channels which were originally used for data annotation. Having these 8 original channels (which were not considered for elimination in the channel selection routine) as a final point, it was assured that all annotated seizures were potentially detectable. The process for SFS was similar.

Results in Fig. 6, which are obtained on one of the largest existing clinical datasets of neonatal EEG, indicate that the proposed data-driven channel weighting increases the performance consistently for different subsets of the chosen channels and different classifier types (discriminative SVM or generative GMM). For the SVM-based system, the performance increase is almost constant across all channels combinations. The average relative improvement in term of the ROC area is 22% (0.74% absolute) for the SVM and 15% (0.68% absolute) for the GMM. It is worth noting that when performance approaches 100%, the performance increase is better perceived in relative terms. An improvement in ROC area from 96.6% to 97.34%, represents a 22% relative increase in performance as only a 3.4% improvement was possible, (97.34-96.6)/(100-96.6).

The channel subset which led to the best performance on the development data and its resulting performance on the testing data for the weighted channel seizure detection schemes are highlighted by the crosses in Fig. 6. For the SVM system (the ROC area is 97.34%), the original 8 channels are augmented by three inter-hemispheric derivations (O2-O1, F4-F3, and C4-C3). For the GMM system (the ROC area is 96.35%), the two channels (F3-C4 and C4-C3) are added to the 8 channels to yield the best development data results. It is interesting to observe that in both systems, the single best channel C3-C4 (Fig. 5) is not the first one to be added to the original subset of 8 channels. This is attributable to the fact that C3 and C4 electrodes are already very well represented in the original 8 channel subset and thus the systems benefit more by augmenting the representation of other electrodes in the final set of channels.

It is also interesting to see the contribution of each of the two terms $P(e|\mathbf{x})$ and $P(e|S)$ in the proposed weighting scheme. This is investigated for the SVM-based system for the operating point (cross) in Fig. 6. The performance of the SVM system without channel weighting is 96.6%. With channel weighting and assuming equal $P(e|S)$ for all electrodes, then the data-driven $P(e|\mathbf{x})$ only influences the final measure and the ROC increases to 97.12%. Moreover, when $P(e|S)$ is defined as in Section IV.B, incorporating clinical information, the performance is further improved to 97.34%. This fact shows that both terms, $P(e|S)$ and $P(e|\mathbf{x})$, are important in the final weight calculation. The proposed measure of channel importance is completely data-driven and computed online, which allows for its usage for other neurological applications which involve EEG monitoring.

C. Per patient performance

To examine which patients benefit most from the proposed weighting, the per-patient absolute difference in the ROC before and after weighting is shown in Fig. 7. This difference is shown for the operating points given in Fig. 6 as these are identifiable without seeing the testing data.

It can be seen from Fig. 7 that the average 22% relative increase in the ROC area for the SVM system is mostly attributable to performance increases in certain patients. Whereas for patients 6, 7, 10, 11, 12, 13, 16, and 17 the channel weighting has no statistically significant effect ($p>0.05$), for the remaining patients p values are close to 0 and hence these indicate significant performance differences for these patients. Increases in ROC for patients 1, 2, 5, and 8 are particularly large. Quantitatively, the ROC areas have been increased from 93.3%

to 96.7%, from 93.5% to 95.1%, and from 92.5% to 98.8% for patients 2, 5, and 8, respectively.

For the GMM system, no statistically significant changes are observed for patients 1, 3, 6, 7, 11, and 16, whereas for the remaining patients p values are close to 0. Performance of patients 2, 5, 10 has been increased from 90.8% to 94.7%, from 92.2 to 94.5%, from 88.1% to 91.1%, respectively.

It is interesting to observe that for both systems the proposed channel weighting has a statistically significant negative effect for patient 4, 9, and 14. Patient 4 has a strong respiration artifact lasting over 3 hours in the F3 electrode which not only causes a false detection but also attenuates other electrodes by mistakenly emphasising the F3 electrode. It can be seen from the patient data given in Table I, that patient 9 has 156 seizures. No improvement has been observed for the other patient with numerous seizures (patient 3, 149 seizures). Apparently, stable weights are not produced over any time interval when seizures are occurring all the time. For patients 14, the observation time is the shortest in the dataset which leads to the same situation. This can also be seen for other patients with short recording times (patient 6, 11, 16, and 17).

The different nature of classifiers employed (discriminative vs. generative) results in the different probabilistic response to seizure and non-seizure patterns. Consequently, the integrated synchrony measure (6) can show different responses for the two systems to suspected seizures. Nevertheless, the pattern of system behaviour for different patients is similar. A thorough analysis of errors of the proposed detector before weighting has been performed in [16] and various sources of misclassification [37] in terms of both missed seizures and false detections have been revealed and discussed. The correlation of the algorithmic performance with the degree of spatial spread of a seizure will be targeted in our future work.

D. Comparison with recently-reported systems

A comparison of results with other studies is complicated by several factors. First, the metrics used to report the results of existing seizure detection systems vary from publication to publication. Some papers only report clinically motivated event-based metrics [3], [5], [33], [36]; others only report epoch-based metrics [34], [35]. Apart from different terms used to name the same metrics across the literature, the comparison of the reported systems is further complicated when only a pair of metric values is reported [3] – [5], [33] – [36] rather than a complete curve of performance of the system [16] – [18], [32]. This fact significantly complicates the comparison of the proposed approaches – one system is usually better according to the first metric and worse according to the second metric. Apart from metrics, some studies report results as an average over training and testing data [34] in contrast to reporting results obtained on testing data only [3], [16], [32], [33]. Others do not have separate testing data at all and report results over the data on which the algorithm was developed [5]. There are numerous papers in the machine learning literature including neonatal seizure detection [36] that show that the performance obtained on the development data is significantly better than the performance obtained on unseen testing data. Averaging over inhomogeneous data also affects performance assessment. In [33] patient-independent and patient-dependent results are averaged. Apart from the fact that the practical usefulness of the patient-dependent seizure detector for neonates is limited, it has also been shown that patient-dependent seizure detection obtains significantly better results. Some report results by averaging over sick and healthy babies [33] in contrast to reporting results separately for each category [3], [5]. In [5] and [23], it has been shown that neonatal seizure detectors produce significantly better performance on healthy babies than on sick babies. Thus, the averaged performance can be made arbitrarily good by increasing the amount of healthy

patient data in the study. Some assess the performance based on a heuristically derived static data division to training and testing datasets [3], [33], [34]. Over-optimistic or indeed over-pessimistic results can be obtained depending on what seems an “arbitrary” partition of the data – a “good” or “bad” split. Others perform more grounded and repeatable statistical tests by dividing the data repeatedly to training and testing [16], [32]. All these different aspects of performance assessment for neonatal seizure detection are discussed in detail in [18].

The comparison is only possible because the curves of performance are reported in our study. Fig. 8 shows a summary of the comparison with the recently reported systems which have been tested on a relatively large datasets using the epoch-based (top) and event-based (bottom) metrics. It can be seen that the proposed system with channel weighting outperforms existing alternatives, and also leads to a performance increase over the similar system without channel weighting which is described in [16]. Quantitatively, the ROC area has been increased from 96.30% to 97.34%. Observing the event-based metrics, it can be seen that at the 0.5 FD/h operating point, the GDR has increased from 82% to 87% which corresponds to an extra ~35 seizures being detected. It is worth noting that the results reported in our work were not increased by averaging over training and testing data, nor by averaging over sick and healthy patients, nor by using a heuristically chosen static data division. Additionally, the dataset contains long recordings of patients with well-defined etiology and gestational age, and therefore is truly representative of the real-life situation in the NICU.

VI. Conclusion

Weighting of channels is proposed for improved neonatal seizure detection. It is shown that the largest benefit in performance is expected in the most difficult clinical situations where it is necessary to detect rare focal events in long term monitoring. The proposed measure of channel importance is completely data-driven and computed online in an unsupervised manner. This allows for its use in other neurological applications which involve EEG monitoring.

Acknowledgments

.This work was supported in part by the Welcome Trust (085249/Z/08/Z) and SFI (10/IN.1/B3036, 07/SRC/I1169)

Biography

Andriy Temko (S’05-M’10) received the Engineering degree in Informatics in 2002 from Dniepropetrovsk National University, Dniepropetrovsk, Ukraine and the PhD degree in Telecommunication in 2008 from Universitat Politècnica de Catalunya (UPC), Barcelona, Spain. His main research interests include kernel methods, signal processing, and multimodal interfaces. Since late 2008 he has been with the Neonatal Brain Research Group, University College Cork, Ireland, working on algorithms for biomedical signal processing and classification.

Gordon Lightbody graduated with the MEng degree (distinction) (1989), and then PhD (1993) both in Electrical and Electronic Engineering from Queen's University Belfast. Since 2008, he has been a Senior Lecturer in Control Engineering at University College Cork. His current research interests include artificial intelligence techniques for intelligent control and signal-processing, focusing on biomedical and energy/power applications.

Eoin M. Thomas received his BE (Electrical and Electronic) in 2006 and his PhD degree in 2011 from University College Cork working on the topic of automated detection of neonatal seizures as part of the Neonatal Brain Research Group. Further topics of interest include EEG classification tasks, event detection and machine learning for biomedical applications.

Geraldine B. Boylan received the M.Sc. degree in physiology and the Ph.D. degree in clinical medicine from University College London, London, U.K. She is currently a Professor of Neonatal Physiology in the Department of Paediatrics & Child health, UCC, Ireland. Much of her recent work is of an interdisciplinary nature and aims to create a synergy between medicine and engineering to address important medical problems such as seizure detection in the neonate.

William Marnane received the B.E. degree in electrical engineering from UCC in 1984, and the Ph.D. degree from the University of Oxford, Oxford, U.K., in 1989. Since 1999, he has been a Senior Lecturer in Digital Signal Processing in the Department of Electrical &

Europe PMC Funders Author Manuscripts

Electronic Engineering at UCC. His research interests include Biomedical Signal Processing and digital design for DSP, coding and cryptography.

References

[1]. Rennie J, Boylan G. Treatment of neonatal seizures. Arch Disease Child. 2007; 92:148–50.

[2]. Murray D, Boylan G, Ali I, Ryan C, Murphy B, Connolly S. Defining the gap between electrographic seizure burden, clinical expression and staff recognition of neonatal seizures. Arch Disease Child. 2008; 93:187–91.

[3]. Mitra J, Glover J, Ktonas P, Kumar A, Mukherjee A, Karayiannis N, Frost J, Hrachovy R, Mizrahi E. A Multistage System for the Automated Detection of Epileptic Seizures in Neonatal Electroencephalography. J Clin Neurophysiol. 2009; 26:1–9. [PubMed: 19151615]

[4]. Celka P, Colditz P. A computer-aided detection of EEG seizures in infants, a singular-spectrum approach and performance comparison. IEEE Tran Biomed Eng. 2002; 49:455–462.

[5]. Deburchgraeve W, Cherian P, Vos M, Swarte R, Blok J, Visser G, Govaert P, Huffel S. Automated neonatal seizure detection mimicking a human observer reading EEG. Clin Neurophysiol. 2008; 119:2447–2454. [PubMed: 18824405]

[6]. Fan J, Shao C, Ouyang Y, Wang J, Li S, Wang Z. Automatic seizure detection based on support vector machines with genetic algorithms. Simulated Evolution and Learning. 2006; 4247:845–852. LNCS.

[7]. Schröder M, Lal T, Hinterberger T, Bogdan M, Hill N, Birbaumer N, Rosenstiel W, Schölkopf B. Robust EEG channel selection across subjects for brain-computer interfaces. EURASIP J App. Sig. Pr. 2005; 19:3103–3112.

[8]. Lan T, Erdogmus D, Adami A, Pavel M, Mathan S. Salient EEG channel selection in brain computer interfaces by mutual information maximization. Proc IEEE EMBC. 2005:7064–7067.

[9]. Lal T, Schröder M, Hinterberger T, Weston J, Bogdan M, Birbaumer N, Schölkopf B. Support vector channel selection in BCI. IEEE Tr Biomed Eng. 2004; 51(6):1003–1010.

[10]. Garipelli G, Chavarriaga R, Cincotti F, Babiloni F, Millán J. Discriminative channel selection method for the recognition of anticipation related potentials from CCD estimated cortical activity. Proc. IEEE MLSP. 2009:1–6.

[11]. Ansari-Asl K, Chanel G, Pun T. A channel selection method for EEG classification in emotion assessment based on synchronization likelihood. Proc. EUSIPCO. 2007:1241–1245.

[12]. Wang Y, Gao X, Gao S. Common spatial pattern method for channel selection in motor imagery based brain-computer interface. Proc. IEEE EMBS. 2005:5392–5395.

[13]. Cecotti H, Gräser A. Convolutional Neural Networks for P300 Detection with Application to Brain-Computer Interfaces. IEEE Trans Pattern Anal Mach Intell. 2011; 33(3)

[14]. Guyon I, Weston J, Barnhill S, Vapnik V. Gene selection for cancer classification using SVMs. Mach Learn. 2002; 46

[15]. Sheth, R. Neonatal Seizures. E-Medicine Pediatric Neurology. http://emedicine.medscape.com/article/1177069-overview, 16/11/2009

[16]. Temko, A.; Thomas, E.; Marnane, W.; Lightbody, G.; Boylan, G. Clin Neurophysiol. Vol. 122. Elsevier; 2011. EEG-based neonatal seizure detection with support vector machines; p. 464-473.

[17]. Thomas E, Temko A, Lightbody G, Marnane W, Boylan G. Gaussian mixture models for classification of neonatal seizures using EEG. Physiol Meas. 2010; 31(7):1047–1064. [PubMed: 20585148]

[18]. Temko, A.; Thomas, E.; Marnane, W.; Lightbody, G.; Boylan, G. Clin Neurophysiol. Vol. 122. Elsevier; 2011. Performance assessment for EEG-based neonatal seizure detectors; p. 474-482.

[19]. Bishop, C. Pattern Recognition and Machine Learning. Springer; 2007.

[20]. Pressler, R.; Binnie, C.; Cooper, R.; Robinson, R. Neonatal and paediatric clinical neurophysiology. 1st ed. Churchill Livingstone Elsevier; Amsterdam: 2007.

[21]. Platt J. Probabilistic outputs for SVM and comparison to Regularized likelihood methods. Advances in Large Margin Classifiers. 1999

[22]. Quigg M, Leiner D. Engineering Aspects of the Quantified Amplitude-Integrated Electroencephalogram in Neonatal Cerebral Monitoring. J Clin Neurophysiol. 2009; 26:145–149. [PubMed: 19424083]

[23]. Temko A, Korotchikova I, Marnane W, Lightbody G, Boylan G. Validation of an automated seizure detection system on healthy babies. Proc. INSTICC/IEEE BioSignals. 2010:312–317.

[24]. Vapnik, V. Estimation of Dependences Based on Empirical Data. Springer-Verlag; New York: 1982.

[25]. Mason S, Graham N. Areas beneath the relative operating characteristics (ROC) and relative operating levels (ROL) curves: Statistical significance and interpretation. Q J R Meteorol Soc. 2002; 128:2145–2166.

[26]. Scher M, Beggarly M. Clinical significance of focal periodic discharges in neonates. J Child Neurol. 1989; 4:175–85. [PubMed: 2504808]

[27]. Shellhaas R, Soaita A, Clancy R. Sensitivity of amplitude-integrated electroencephalography for neonatal seizure detection. Pediatrics. 2007; 120:770–777. [PubMed: 17908764]

[28]. Shellhaas R, Clancy R. Characterization of neonatal seizures by conventional EEG and single-channel EEG. Clin Neurophysiol. 2007; 118(10):2156–2161. [PubMed: 17765607]

[29]. Wusthoff C, Shellhaas R, Clancy R. Limitations of single-channel EEG on the forehead for neonatal seizure detection. J Perinatol. 2009; 29:237–242. [PubMed: 19052554]

[30]. Bourez-Swart M, van Rooij L, Rizzo C, de Vries L, Toet M, Gebbink T, Ezendam A, van Huffelen A. Detection of subclinical electroencephalographic seizure patterns with multichannel amplitude-integrated EEG in full-term neonates. Clin Neurophysiol. 2009; 120(11):1916–1922. [PubMed: 19782640]

[31]. Guyon I, Elisseeff A. An Introduction to Variable and Feature Selection. J Mach Learn Res. 2003; 3:1157–1182.

[32]. Greene B, Marnane W, Lightbody G, Reilly R R, Boylan G. Classifier models and architectures for EEG-based neonatal seizure detection. Physiol Meas. 2008; 29:1157–1178. [PubMed: 18799836]

[33]. Navakatikyan M, Colditz P, Burke C, Inderd T, Richmond J, Williams C. Seizure detection algorithm for neonates based on wave-sequence analysis. Clin Neurophysiol. 2006; 117:1190–1203. [PubMed: 16621690]

[34]. Aarabi A, Grebe R, Wallois F. A multistage knowledge-based system for EEG seizure detection in newborn infants. Clin Neurophysiol. 2007; 118:2781–2797. [PubMed: 17905654]

[35]. Liu A, Hahn J, Heldt G, Coen R. Detection of neonatal seizures through computerized EEG analysis. Electroencephalogr Clin Neurophysiol. 1992; 82:30–37. [PubMed: 1370141]

[36]. Gotman J, Flanagan D, Zhang J, Rosenblatt B. Automatic seizure detection in the newborn: methods and initial evaluation. Electroencephalogr Clin Neurophysiol. 1997; 103(3):256–62.

[37]. André M, Lamblin M, d'Allest A, et al. Curzi-Dascalova L, Moussali-Salefranque F, Nguyen S, Vecchierini-Blineau M, Wallois F, Walls-Esquivel E, Plouin P. Electroencephalography in premature and full-term infants. Developmental features and glossary. Clin Neurophysiol. 2010; 40(2):59–124.

[38]. Hanley J, McNeil B. A method of comparing the areas under receiver operating characteristic curves derived from the same cases. Radiology. 1983; 148(3):839–843. [PubMed: 6878708]

Europe PMC Funders Author Manuscripts

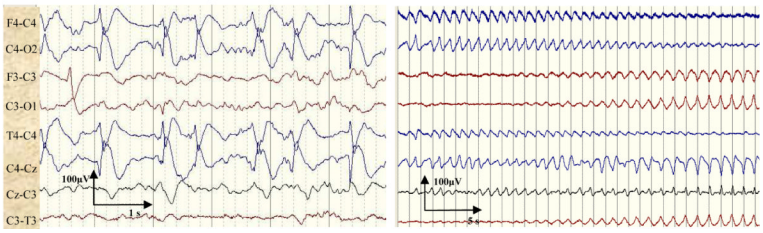

Fig. 1.

Neonatal seizures. Left graph shows an example of a focal seizure localized in the C4 electrode zone. Right graph shows an example of seizure migration from C4 to C3.

Europe PMC Funders Author Manuscripts

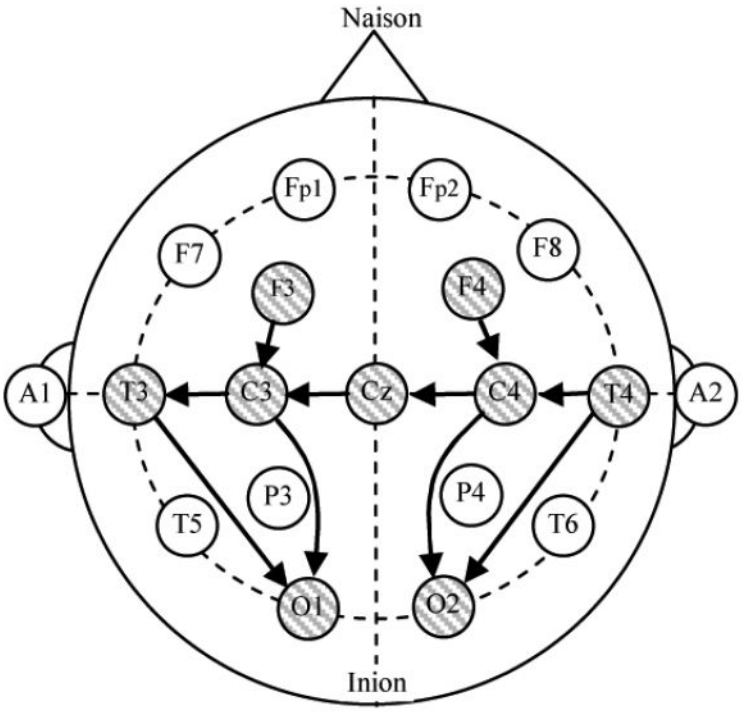

Fig. 2.

The conventional 10-20 electrode placement modified for neonates. The following 9 electrodes were used to record the data in our work: T4, T3, O1, O2, F4, F3, C4, C3, and Cz. The following 8 channels in bipolar montage were used to annotate the data: F4-C4, C4-O2, F3-C3, C3-O1, T4-C4, C4-Cz, Cz-C3 and C3-T3.

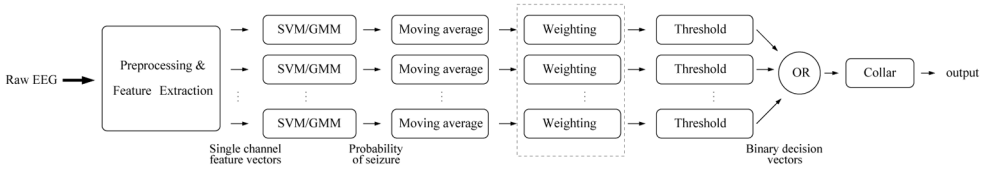

Fig. 3.

Neonatal seizure detector system diagram. The weighting of the probabilistic outputs of the primary classifiers is highlighted.

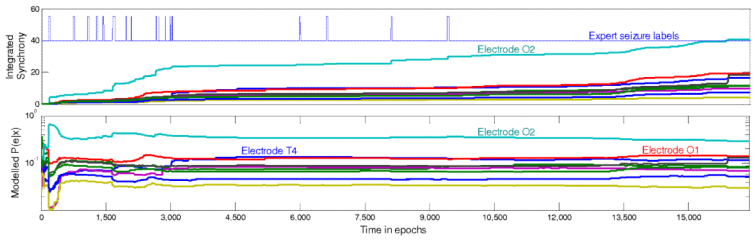

Fig. 4.

An example of the proposed measure of electrode importance calculated for patient 1. The top graph shows the integrated synchrony for each electrode with the superimposed expert seizure labels. The bottom graph plots the resultant $P(e|x)$. The emphasis of the electrode O2 increases during ictal activity.

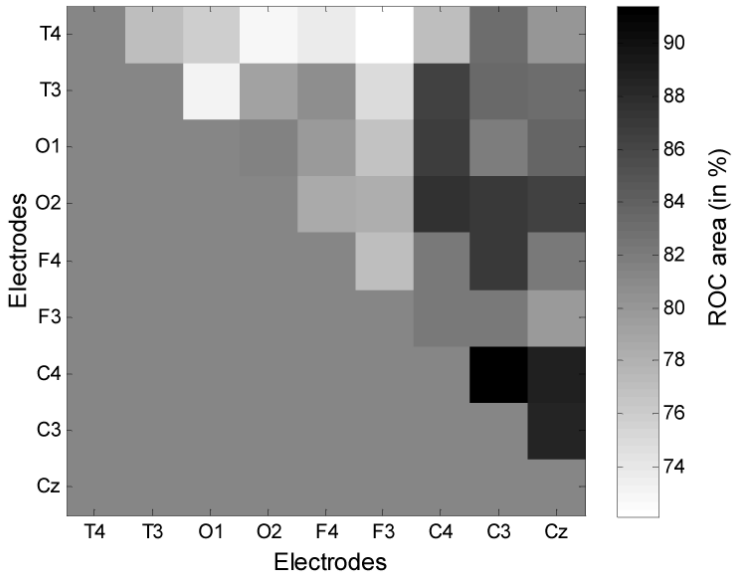

Fig. 5.
Performance of the SVM-based seizure detection system for every possible channel in bipolar montage with 9 electrodes available.

Europe PMC Funders Author Manuscripts

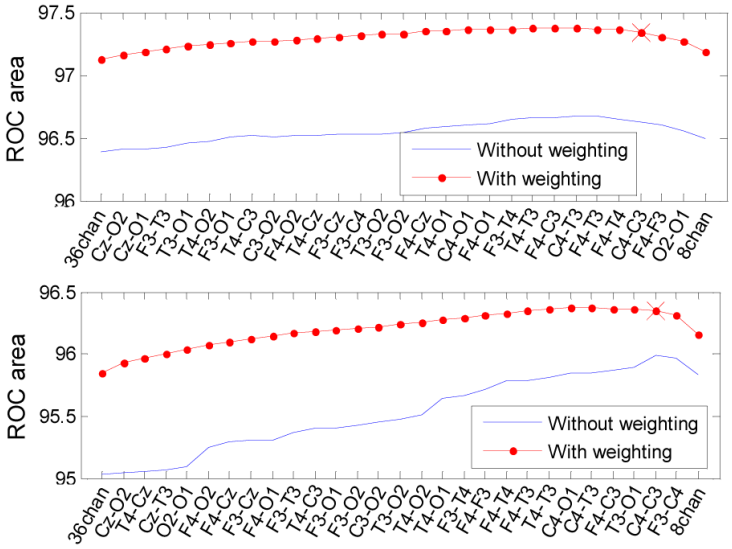

Fig. 6.

Performance of the SVM-based (top) and GMM-based (bottom) seizure detection systems with and without channel weighting for various channel combinations selected by SBE/SFS. This procedure provides nested subsets of channels. The x-axis indicates the difference between two adjacent channel subsets.

Europe PMC Funders Author Manuscripts

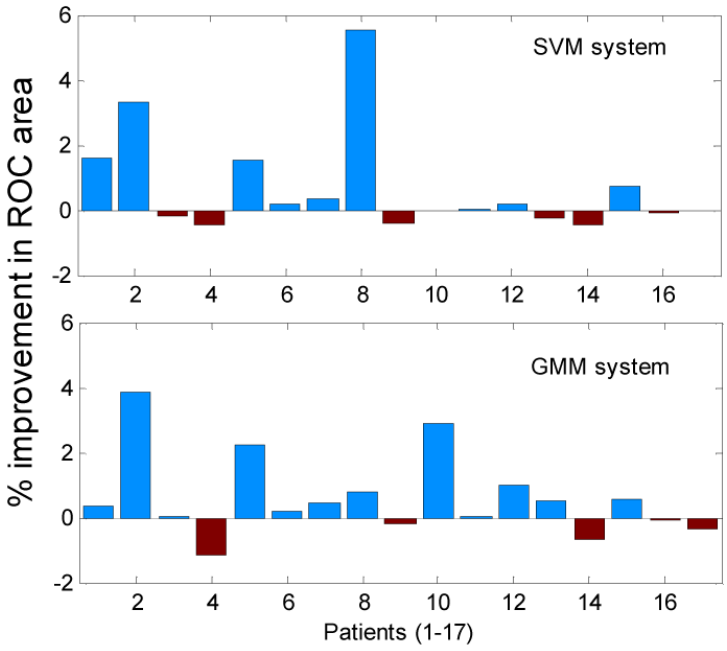

Fig. 7.
Per-patient improvement (absolute) in ROC areas for the SVM-based (top) and GMM-based (bottom) detectors obtained using channel weights.

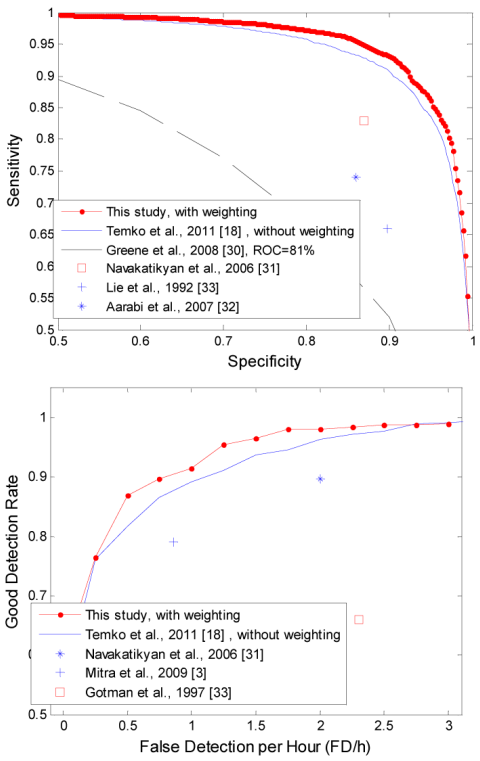

Fig. 8.
A comparison with recently reported systems using the epoch-based (top) and event-based (bottom) metrics.

Europe PMC Funders Author Manuscripts

Europe PMC Funders Author Manuscripts

TABLE I

EEG Dataset

Patient	Record length (h)	Seizure events	Mean Seizure Duration	Min Seizure Duration	Max Seizure Duration
1	18.23	17	1′30″	17″	3′54″
2	24.74	3	6′10″	55″	11′09″
3	24.24	149	2′18″	10″	10′43″
4	26.10	60	1′03″	25″	1′46″
5	24	49	5′54″	21″	31′01″
6	5.69	41	1′09″	26″	1′53″
7	24.04	6	1′04″	18″	1′28″
8	24.53	17	5′57″	29″	19′14″
9	24.04	156	5′16″	16″	37′06″
10	10.06	25	5′26″	10″	21′22″
11	6.19	15	5′26″	26″	7′49″
12	12	29	2′11″	13″	6′24″
13	12.13	25	4′06″	71″	12′16″
14	5.48	11	8′34″	69″	30′36″
15	12.16	59	2′05″	11″	7′08″
16	7.63	31	10′23″	2′14″	34′37″
17	6.64	12	8′32″	44″	23′16″
Total	**267.9**	**705**			

Europe PMC Funders Author Manuscripts

TABLE II

Features Extracted For Each Epoch

- Total power (0-12Hz), - Peak frequency of spectrum, - Spectral edge frequency (SEF80%, SEF90%, SEF95%), - Power in 2Hz width subbands (0-2Hz, 1-3Hz, …10-12Hz), - Normalised power in same subbands, - Db4 wavelet coefficient corresponding to 1-2Hz)
- Curve length, - Number of maxima and minima, - Root mean square amplitude, - Hjorth parameters (activity, mobility and complexity), - Zero Crossing Rate (ZCR), - ZCR of the Δ and the ΔΔ, - Variance of Δ and ΔΔ, - Autoregressive modelling error (AR model order 1-9), - Skewness, - Kurtosis, - Nonlinear energy
- Shannon entropy, - Spectral entropy, - Singular Value Decomposition entropy, - Fisher information

Europe PMC Funders Author Manuscripts

TABLE III

Channels Used For Modelling Electrode Importance

Electrode	Channels used
T4	T4-O2, F4-T4, T4-C4
T3	T3-O1, F3-T3, C3-T3
O1	T3-O1, C3-O1, Cz-O1, O2-O1
O2	T4-O2, C4-O2, Cz-O2, O2-O1
F4	F4-T4, F4-C4, F4-Cz, F4-F3
F3	F3-T3, F3-C3, F3-Cz, F4-F3
C4	T4-C4, F4-C4, C4-O2, C4-Cz, C4-C3
C3	C3-T3, F3-C3, C3-O1, Cz-C3, C4-C3
Cz	F4-Cz, F3-Cz, C4-Cz, Cz-C3,Cz-O1, Cz-O2

TABLE IV

P(E|S) Modeled From Statistics Given in Clinical Literature

Electrode	T4	T3	O1	O2	F4	F3	C4	C3	Cz
P(e/S)	0.46	0.46	0.46	0.46	0.46	0.46	0.78	0.78	0.94